ELSEVIER

Advances in defining fine- and micro-scale pattern in marine plankton

Dale V. Holliday [a,*], Percy L. Donaghay [b], Charles F. Greenlaw [a], Duncan E. McGehee [a],
Margaret M. McManus [c], Jim M. Sullivan [b], Jennifer L. Miksis [b]

[a] *BAE SYSTEMS, 4669 Murphy Canyon Road, San Diego, CA 92123, USA*
[b] *University of Rhode Island, Graduate School of Oceanography, Narragansett, RI 02882, USA*
[c] *University of California at Santa Cruz, Santa Cruz, CA 95064, USA*

Abstract

Since the June 1995 ICES Symposium on Fisheries and Plankton Acoustics in Aberdeen (MacLennan and Holliday, 1996), the use of acoustics for studying zooplankton has seen important advances. Acoustical monitoring of small-scale zooplankton distributions can now be done at intervals of a fraction of a minute. Resolution at vertical spatial scales of tens of centimeters is now easily achieved with commercially available sensors. Multiple-frequency echo-ranging sensors (TAPS™) have been deployed in an up-looking mode on the bottom, and on moorings looking up, down and horizontally. Real-time telemetry provides data on plankton distributions at ranges up to tens of meters from the sensors for periods of weeks to months. These sensors allow one to estimate total zooplankton biomass and the size-abundance spectrum of the animals in the water column at different depths and times. When a profiling CTD and multi-spectral optical sensors were used to define the physical environment and phytoplankton distributions near an acoustical zooplankton profiler, strong relationships were observed between measured spatial and temporal patterns. New methods in zooplankton acoustics are illustrated with data collected from these sensors while monitoring thin, sub-meter thick layers of plankton and diel migrations of benthopelagic crustaceans.

1. Introduction

Since the mid-1990s, major improvements have been achieved in measuring fine- and micro-scale distributions of both phytoplankton and zooplankton. Advances have been made in using optical sensors to determine the distribution and characteristics of phytoplankton (primary producers). Advances continue to be made using optical techniques in studying phytoplankton, e.g., measurement of inherent and apparent optical water column properties using both multi- and hyper-spectral sensors (Twardowski et al., 1999) and flow cytometry for characterizing individual cells (Jochem, 2000). Striking advances have also been made in estimating the biomass, spatial distribution and temporal dynamics of assemblages of secondary producers, i.e., the zooplankton and micronekton. These advances stem largely from the evolution of multi-frequency acoustical sensors and from improvements in theory for describing scattering from small

particles. Both marine optics and acoustics have also benefited from innovative changes in the way we deploy such instruments and from advances in theoretical descriptions of scattering and propagation.

2. Background and motivation

Even with the best technology of the late 20th century, it was a challenge to detect fine- and micro-scale spatial structure in the sea, much less to quantify it by describing the relationships between phytoplankton, zooplankton, and relevant small-scale physical features in the ocean. The vertical resolution of our best cast-deployed physical, chemical, acoustical, and optical sensors was limited by coupling of the wave and swell induced meter-scale vertical motions of a ship to an instrument or direct sampling device over periods of a few seconds. As sensor technologies and deployment modes evolved, we have finally begun to detect and describe some of the micro- and fine-scale structures that fisheries and plankton ecologists (Cassie, 1963; Lasker, 1975; Mullin and

Brooks, 1976) inferred from trophic arguments. We now describe and even monitor ecologically critical small-scale features in phytoplankton and zooplankton distributions which have been at best seriously under-sampled and often completely missed. We can now reveal patterns in primary and secondary producers at scales sampled adequately in both time and space, i.e., we can measure at scales that are not necessarily aliased by the sampling process (Platt and Denman, 1975). Sensors with high accuracy, resolution and precision can reveal zooplankton biomass and size spectra at tens of centimeters in the vertical, with horizontal resolutions of about a meter, and with temporal resolutions of better than a minute, for months. Modern acoustical zooplankton sensors have revealed that over 75% of the zooplankton biomass can be concentrated in a few sub-meter thick "thin layers" in a 50 m water column (Holliday, 1998). Similar "thin layer" vertical structures in physical, chemical and phytoplankton distributions have also been described (Donaghay et al., 1992; Cowles and Desiderio, 1993; Hanson and Donaghay, 1998). If, as Lasker and Mullin pointed out in the late 1960s, you are a fish larva, you may indeed be fortunate to find such a food resource.

We offer examples of data from studies where we have deployed instrumentation to allow high-resolution studies of fine- and micro-scale structures. These are scales, in both time and space, but especially in depth, which are relevant to the experiences of an individual organism. These tools are not only useful for small-scale work but have also been applied to problems that span hundreds of kilometers (McGehee et al., 2000; Pieper et al., 2001). Here, however, we focus on applications at small scales.

3. Evolutions in the modeling of acoustical scattering

In addition to advances in acoustical sensor technology, there have been important developments in mathematical modeling of acoustical scattering and in the software used to convert volume scattering data into measures that reflect the biophysical character of the scatterers and their distribution in relation to their environment.

During the late 1990s, the most widely used models of scattering from zooplankton and micronekton were analytical, the most useful being those of Anderson (1950), Faran (1951), Stanton (1988, 1989, 1990) and Stanton and Chu (1992). Simple adaptations of these models, such as the high-pass fluid sphere model (Johnson, 1977, 1978), the truncated versions of the fluid and elastic spheres (Holliday, 1992, 1987) were also available. While the stimulus for the newest models for scattering from zooplankton can often ultimately be traced to Stanton, through his students and research collaborators, the newest generation of models is largely numerical.

One such model involves the use of the Distorted Wave Born Approximation (DWBA). It was first implemented for micronekton in the late 1990s (McGehee et al., 1998; Martin-Traykovski et al., 1998) in 2-D, and in 3-D by Lavery and her
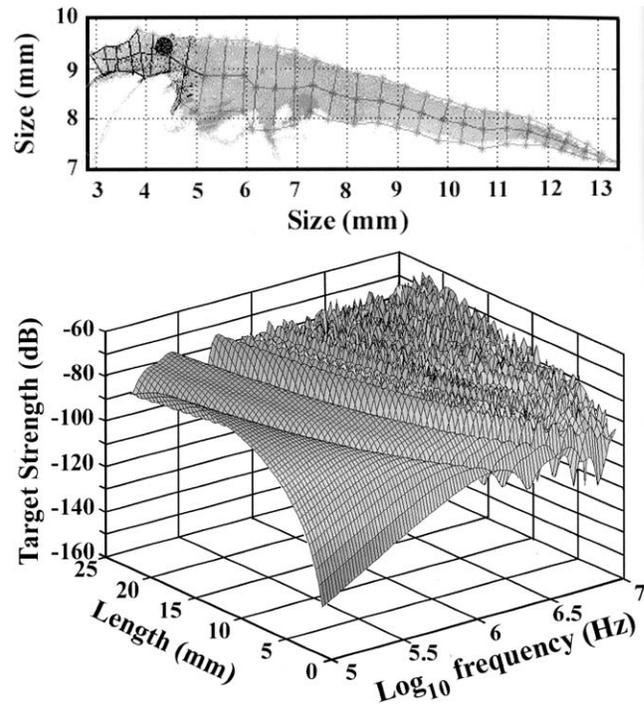

Fig. 1. Predicted ventral aspect scattering from a mysid. See McGehee et al., 1998 for details of modeling method.

collaborators (Lavery et al., 2002). In these models, the silhouettes (2-D) and volumes (3-D) of zooplankters are obtained photographically or via computerized tomography (CT-scans). Numerical integration yields estimates of scattering for realistic animal shapes at different sizes and selected orientations with respect to the incident sound waves.

To illustrate one of the new modeling techniques, the perimeter of a mysid was approximated by a series of cylinders whose radii were positioned orthogonally with respect to the central axis of the animal (Fig. 1, top panel). The dependence of the ventral target strength on animal length and the acoustic frequency, as computed with a 2-D DWBA model revealed a complex dependence of target strength on the acoustic frequency and the length of the mysid including both Rayleigh and geometric scattering domains (Fig. 1, bottom panel).

The shape of this mysid is similar to that of several common species of euphausiids. The ventral aspect angle was used to support an analysis of data where the acoustical system "looked" upward. Mysids have been observed swimming naturally in the approximate aspect illustrated (P. Jumars, pers. comm.).

4. Advances in inversion processing

Given accurate models of the scatterers in the water column and good multi-frequency estimates of acoustical volume scattering strength, one can estimate zooplankton abundance vs. size for each time-depth resolution cell (pixel) in a

sequence of echo-ranging profiles. Although the principles for multi-model inversion were outlined by Holliday (1977), implementation of the multi-frequency, multi-model process was not attempted in earnest until the late 1990s when modeling of scattering from animals of different morphologies had substantially advanced. Current versions of inverse codes optimally and simultaneously apportion the energy in the acoustic volume scattering strength spectra for each time and depth interval (pixel) into an estimated size-biomass spectrum for each scattering model supplied by the user.

5. Improvements in resolution of small-scale structure

Vertical spatial resolutions achievable in the mid-1990s were nominally >2 m, but are now ~0.125 m. From ships making stations along a transect, we were limited to making vertical casts about once an hour. With moored sensors in the coastal zone, we now routinely sample a 20–30 m water column at 0.5 min intervals, or better. Previously, casts along a transect from a ship were spaced at horizontal intervals not less than ~500 m. The surface footprint of an up-looking moored sounder at 20 m depth today resolves horizontal structure at ~1 m scales as the water is advected over the sensor. Similar horizontal resolutions could be achieved from moving platforms in an "echo sounder" mode. Data acquired with traditional research cruises on ships often span only a few days or weeks, often missing important variations in the distribution of biomass on both shorter and longer intervals of time, e.g., details of diel migrations, the responses of biota to storms, seasonal, and even annual changes. Data collected with today's multi-frequency moored acoustical zooplankton sensors may span several months at sampling intervals of less than a minute. With fairly minimal maintenance, e.g., removal of biological fouling on the sensors, even longer periods are entirely practical in some situations. This presents both an opportunity and a challenge. The opportunity involves being able to watch a distribution evolve and change on scales similar to the ambit and life-span of an individual zooplankter. The challenge involves the fact that the amount of data one must archive, process, visualize, correlate with environmental and trophic data at similar scales, and then interpret, is sometimes overwhelming.

Depending on the science objective of the deployment, we have arranged the sensors to look either up into the water column above them, or down to study the benthopelagic fluxes in the water column just above the seabed (Richardson et al., 2001). Volume scattering strength profiles can be reported at multiple acoustical frequencies, averaged over multiple echo-ranging cycles, at intervals of as often as every 30 s for months. As we have currently configured our acoustical sensor packages, a limited amount of internal sensor storage is available, but normally data are telemetered to a shore station via a spread spectrum radio with line-of-sight distances of about 30 km. This data link may also be used to remotely control a variety of sensor operating parameters. When it is desirable to use the system for more than about

3 weeks without changing the batteries, the system can be deployed at the end of an ~1 km cable, supplying power from shore and enabling two way communications.

To illustrate the difference these technological improvements have made, we use data from a TAPS deployment in a shallow fjord in northern Puget Sound, located between Seattle, WA, USA and Victoria, BC, Canada (Fig. 2). During the summer of 1998, the authors deployed several multi-frequency acoustical zooplankton sensors (TAPS™) on anchored sub-surface buoys. This sensor measured volume scattering strengths at 265, 420, 700, 1100, 1850 and 3000 kHz with a 12.5 cm range resolution with a set of approximately six° beams that insonify a common volume between the depth of a moored mid-water float and the surface. The maximum effective range for any active acoustical sensor depends on the abundance and kinds of scatterers in the water column and the acoustic frequency. In typical applications in the coastal ocean we have obtained useful results with the TAPS at ranges up to 20 or 30 m.

The differences between the spatial and temporal resolutions available from zooplankton acoustical sensors in the mid-1990s and today are graphically illustrated (Fig. 2, bottom panel) with data from an up-looking TAPS at the resolution available in 1998 (1 min, 0.125 m vertical). The high resolution (1998) data were re-sampled at the temporal and vertical spatial resolutions available in 1994 (1 h, 2 m vertical) to duplicate the aliasing that would have resulted from the lower sampling densities and a comparison illustrates the improvements achieved. Clearly, the higher resolution representation of the data conveys far more detail than was available less than a decade ago.
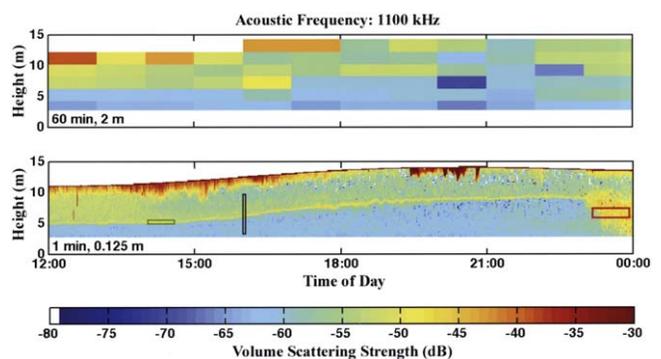

Fig. 2. An up-looking sounder record at 1.1 MHz was collected on June 25, 1998 in East Sound, Orcas Is., WA, USA. This record (lower panel) has been re-sampled once an hour and at 2 m intervals in depth (upper panel). The lower sampling density would have been comparable to the state-of-the-art in 1994 and illustrates the benefits of increases in resolution of acoustical volume scattering strengths measured from a mid-water mooring. The highest resolution data (bottom panel) reveal extensive detail of fine- and micro-scale structures in the water column during a 12-h period. The data in the upper panel is clearly under-sampled, and is aliased, causing major features to be missed or underestimated. It reveals little about the plankton fine structure. The "boxes" define specific times and depth ranges that are further discussed in the text.

6. Relating structure in biomass and environment

One obvious feature of this data set was the very thin layer of high acoustical scattering observed 5 m above the TAPS at noon (Fig. 2, bottom panel). This scattering layer shoaled slowly during the following 11 h. An autonomous winch which carried a CTD and sensors for O_2 and optical absorption was moored ~5 m from the TAPS and collected profiles once an hour. At 16:00 Pacific Daylight Time (PDT), the acoustical scattering layer was located 6.2 m above the TAPS, midway between the oxycline and the pycnocline (Fig. 3, arrow b). An O_2 minimum (3.8 ml l^{-1}) coincided with the scattering layer. Above the oxycline, O_2 levels were supersaturated by ~20%, while O_2 values below the pycnocline were well below saturation. Near the surface, bubbles, possibly generated by high phytoplankton production and brought out of the supersaturated solution by solar heating were episodically advected downward into the water column by Langmuir circulation during this period by light, variable (<4 m/s) winds. The acoustic spectra and scattering levels in the plumes near the surface (Fig. 2) are consistent with the presence of very small bubbles. At the same time, a thin (0.14 m) optical absorption layer was detected 7.1 m above the TAPS, or 0.9 m above the pycnocline and its associated zooplankton scattering layer. This thin optical layer, characterized by a peak total optical absorption value (a_{pg}) of 3.7 m^{-1} at 440 nm, was co-located with an O_2 maximum (7.2 ml l^{-1}). Sampling with a siphon revealed that it was due to phytoplankton. The acoustical scattering layers were only 22.5–45.0 cm thick for most of this particular 12-h period. A small packet of internal waves, with peak-to-peak amplitudes of less than a meter appeared at about 17:30 PDT, modulating the depth of the pycnocline and the acoustical scattering layer for about 2 h.

We illustrate the multi-model inverse method with three selections from the high resolution data of Fig. 2 (bottom panel). We employed two scattering models. The first was the
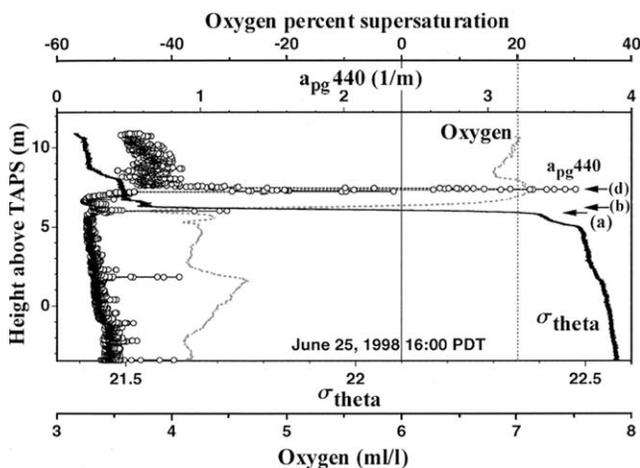
truncated fluid sphere model often used as a generic description of scattering for small crustaceans such as copepods and amphipods (Costello et al., 1989). The second model was the DWBA elongate model of Fig. 1, chosen because *Neomysis* was collected during our occupation of this site and this organism often dominates nighttime emergence trap collections in this environment. Our inverse code optimally and simultaneously apportions the energy in the acoustic volume scattering strength spectra for each selected time and depth interval (pixel) into sizes supplied by the user with methods originally described by Holliday (1977).

An inverse calculation for pixels at the times and depths in the "box" on the thin scattering layer (Fig. 2, bottom panel, ~14:00 h) revealed that the layer was dominated by small copepod-size crustaceans averaging 1.2 mm total length. Several additional sizes were characterized by each of the modeled shapes (Fig. 4), but each with lesser biovolumes relative to the copepod-size animals.

The leftmost "box" in Fig. 2 included 220 independent estimates of volume scattering at each of five frequencies, spanned a 40-min time interval and 0.625 m in depth. Similar calculations revealed that the assemblage of small copepod-like scatterers just above and just below the layer at the same time were similar in size and relative abundance to those in the layer. This suggests that the layer was formed by aggregation of nearby small crustaceans—on the pycnocline in this instance. Average biovolumes of copepod-like organisms in the layer were ~300 mm^3 m^{-3}, while the biovolumes in the upper mixed layer averaged ~100 mm^3 m^{-3}. Immediately below the pycnocline, and to depths extending to ~2 m above the bottom, the copepod-size biovolumes averaged only ~15–20 mm^3 m^{-3}.

Acoustical data collected during the hourly CTD/optics profile (center "box", Fig. 2) were also examined with the two-model inverse code, revealing details of the fine-scale depth distribution of the different shapes and sizes of zooplankters in relation to their environment (Fig. 5). A layer of small "fluid-sphere-like" scatterers were bounded by the steepest point on the pycnocline (a) from below and by the oxycline (b) from above. Lesser concentrations of copepod-size scatterers were found above, but few were observed below the layer on the thermocline. The depth of the maxi-
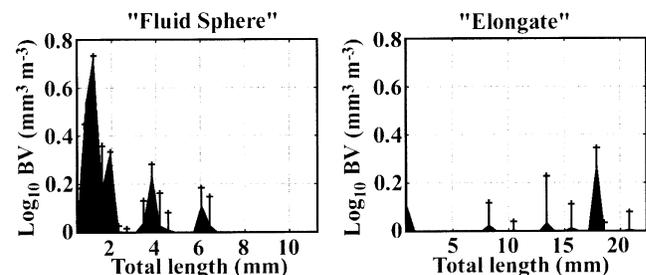

Fig. 3. σ_{theta}, O_2, percent supersaturation of O_2, and a_{pg} at 440 nm vs. depth at 16:00 PDT. Measurements are relative to the TAPS (0 m) which was moored at 20.6 m depth (MLLW). The locations marked (a), (b) and (d) are discussed in the legend for Fig. 5.

Fig. 4. Logarithmic biovolume spectra for thin layer averaged over all the time and depth pixels included in the green "box" in Fig. 2. Average biovolumes are defined by the top edge of the shaded areas while the mean plus one standard deviation of the biovolume is indicated by the vertical lines with the "+" at the top.
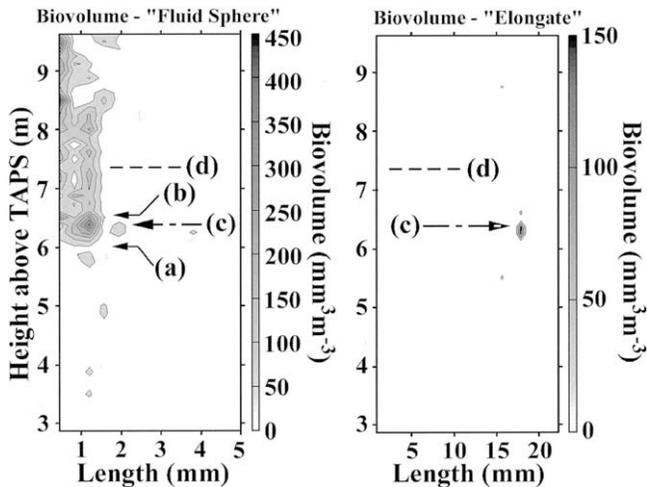
Fig. 5. Biovolume distributions for two distinct shapes of organisms at 16:00 PDT, June 25, 1998. The mid-point of the seasonal pycnocline (a); the mid-point of the oxycline (b); the mid-depth for 1.2 mm long copepods (c); and the depth of a thin layer of optically detected phytoplankton (d) are indicated. Contours are at intervals of 20 mm³ m⁻³.

mum of this small crustacean distribution (c) was consistently just above that of the larger mysid-shaped (elongate) animals concentrated in a separate, but adjoining thin layer (<1 m thick) immediately below the seasonal thermocline. During the time designated by the center "box" (Fig. 2), peaks at several different sizes from ~7–22 mm total length were present, with biovolume peaks at different sizes reaching to as high as 180–200 mm³ m⁻³.

The acoustically determined size distributions for organisms located just below the pycnocline were consistent with the presence of several distinct cohorts (stages) of mysids, similar in size structure and abundance to an assemblage independently observed earlier in a nearby fjord (West Sound) on the same island. At 16:00 PDT, however, only one size of the elongate scatterers was present at significant levels above 20 mm³ m⁻³ (the contour interval). The thin layer of small crustaceans was at the shallow O_2 minimum (3.8 ml l⁻¹) and a second O_2 minimum (~4.1 ml l⁻¹) was observed at the depth of the larger mysid-shaped elongate animals. There was little evidence of small or large crustaceans scattering sound at the depth of the thin optical layer of phytoplankton (Fig. 5) during the daylight hours.

At the latitude of East Sound, the sun sets late during June. Sunset was at 21:17 PDT and nautical twilight ended at 23:00 PDT on the 25th. An increase in scattering at nautical twilight (Fig. 2) was consistent with the migration of several sizes of elongate scatterers to mid-water depths. Results of multi-model inverse calculations averaged over 504 pixels from below the layer after sunset (right 'box", Fig. 2) allows attribution of the increased nighttime scattering to larger organisms with both sphere-like and elongate shapes (Fig. 6).

7. Conclusions

Our ability to examine zooplankton in the coastal ocean has changed dramatically for the better during the last de-
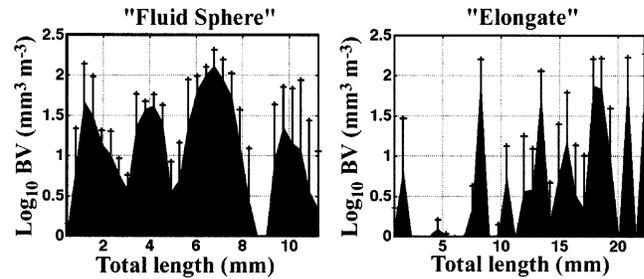

Fig. 6. Logarithmic biovolume spectra for thin layer averaged over all the time and depth pixels included in the red "box" on the right in Fig. 2.

cade. Likewise, there have been major advances in sampling the physics, chemistry and the phytoplankton. Advanced telemetry and new modeling and computing assets suggest a need to consider how we will display so much data and how we can "see" it in ways that will lead to identification of causes and effects, e.g., behavior.

Acoustical and optical methods can now be used to describe how some plankton distributions are related to fine-scale ocean physics and chemistry. Indeed, acoustics and optics are increasingly being used by investigators internationally to address their own science interests. The ability to observe plants and animals nearly continuously and with ever increasing spatial resolution, combined with future deployments on new, novel platforms, should accelerate the rate at which we learn how life survives, and even thrives, in the sea. It is also clear that making observations for sufficiently long periods to allow observation of the marine equivalent of the rare, but critical, terrestrial forest fire is needed. Technology, driven by external forces such as consumer electronics, is moving to lower power requirements, increased storage and improved data telemetry. These developments allow us to observe, at least at points in the ocean, for months now and likely for much longer—e.g., years or decades—in the future.

Finally, we are at the beginning of our exploration of acoustics and optics for studying zooplankton and phytoplankton. Improvements in modeling of scattering in both fields, doing inverse computations, and development of novel, enabling modes of deployment for a multitude of sensors are on the "drawing boards". Completely new approaches, such as multi-static, multi-frequency acoustics have not yet been developed for field use, but are being addressed. This is an iterative process, requiring both experiment and theoretical developments. It sometimes requires starting in the lab, going to sea, learning, going back to the lab. This approach rewards cooperating scientists with diverse heritages (e.g., physicists and biological oceanographers) who are interested in learning the language of other disciplines.

References

Anderson, V.C., 1950. Sound scattering from a fluid sphere. J. Acoust. Soc. Am. 22, 426–431.

Cassie, R.M., 1963. Microdistribution of plankton. Oceanogr. Mar. Biol. Ann. Rev. 1, 223–252.

Costello, J.H., Pieper, R.E., Holliday, D.V., 1989. Comparison of acoustic and pump sampling techniques for the analysis of zooplankton distributions. J. Plankton Res. 11, 703–709.

Cowles, T.J., Desiderio, R.A., 1993. Resolution of biological microstructure through in situ fluorescence emission spectra. Oceanography 6, 105–111.

Donaghay, P.L., Rines, H.M., Sieburth, J.M., 1992. Simultaneous sampling of fine scale biological, chemical and physical structure in stratified waters. Arch. Hydrobiol. 36, 1–14.

Faran, J.J., 1951. Sound scattering by solid cylinders and spheres. J. Acoust. Soc. Am. 23, 405–418.

Hanson Jr., A.K., Donaghay, P.L., 1998. Micro to fine scale chemical gradients and layers in vertically stratified coastal waters. Oceanography 11, 10–17.

Holliday, D.V., 1977. Extracting bio-physical information from the acoustic signatures of marine organisms. In: Anderson, N.R., Zahuranec, B.J (Eds.), Ocean Sound Scattering Prediction, vol. 5. Plenum Press, Marine Science Series, New York, pp. 619–624.

Holliday, D.V., 1987. Acoustic determination of suspended particle size spectra. In: Kraus, N.C (Ed.), Proceedings of a Specialty Conference on Advances in Understanding of Coastal Sediment Process, Coastal Sediments - 1987, vol. 1. American Society of Civil Engineers, New York, pp. 260–272.

Holliday, D.V., 1992. Zooplankton acoustics. In: Desai, B.N (Ed.), Oceanography of the Indian Ocean. Oxford and IBH Publishing Co. Pvt. Ltd., New Delhi, pp. 733–740.

Holliday, D.V., 1998. Acoustical sensing of small-scale vertical structures in zooplankton assemblages. Oceanography 11, 18–23.

Jochem, F.J., 2000. Probing the physiological state of phytoplankton at the single-cell level. Sci. Mar. 64, 183–195.

Johnson, R.K., 1977. Sound scattering from a fluid sphere revisited. J. Acoust. Soc. Am. 61, 375–377.

Johnson, R.K., 1978. Erratum: sound scattering from a fluid sphere revisited. J. Acoust. Soc. Am. 63, 626.

Lasker, R., 1975. Field criteria for survival of anchovy larvae: the relation between inshore chlorophyll maximum layers and successful first feeding. Fish Bull. 73, 453–462.

Lavery, A., Stanton, T.K., McGehee, D.E., Chu, D., 2002. Three-dimensional modeling of acoustic backscattering from fluid-like zooplankton. J. Acoust. Soc. Am. 111, 1197–1210.

MacLennan, D.N., Holliday, D.V., 1996. Fisheries and plankton acoustics: past, present, and future. ICES J. Mar. Sci. 53, 513–516.

Martin-Traykovski, L.V., O'Driscoll, R.L., McGehee, D.E., 1998. Effect of orientation on broadband acoustic scattering of Antarctic krill *Euphausia superba*: implications for inverting zooplankton spectral acoustic signatures for angle of orientation. J. Acoust. Soc. Am. 104, 2121–2135.

McGehee, D.E., O'Driscoll, R.L., Martin-Traykovski, L.V., 1998. Effect of orientation on acoustic scattering from Antarctic krill at 120 kHz. Deep-Sea Res. 45, 1273–1294 (Part II).

McGehee, D.E., Greenlaw, C.F., Holliday, D.V., Pieper, R.E., 2000. Multi-frequency acoustical volume backscattering patterns in the Arabian Sea - 265 kHz to 3 MHz. J. Acoust. Soc. Am. 107, 193–200.

Mullin, M.M., Brooks, E.R., 1976. Some consequences of distributional heterogeneity of phytoplankton and zooplankton. Limnol. Oceanogr. 21, 784–796.

Pieper, R.E., McGehee, D.E., Greenlaw, C.F., Holliday, D.V., 2001. Acoustically measured seasonal patterns of zooplankton in the Arabian Sea. Deep-Sea Res. 48, 1325–1343 (Part II).

Platt, T., Denman, K., 1975. Spectral analysis in ecology. Ann. Rev. Ecol. Systemat. 6, 189–210.

Richardson, M.D., Briggs, K.B., Bibee, L.D., Jumars, P.A., Sawyer, W.B., Albert, D.G., Bennett, R.H., Berger, T.K., Buckingam, M.J., Chotiros, N.P., Dahl, P.H., Dewitt, N.P., Fleischer, P., Food, R., Greenlaw, C.F., Holliday, D.V., Hulbert, M.G., Hutnak, M.P., Jackson, P.D., Jaffe, J.S., Johnson, H.P., Lavoie, D.L., Lyons, A.P., Martens, C.S., McGehee, D.E., Moore, K.D., Orsi, T.H., Piper, J.N., Ray, R.I., Reed, A.H., Self, R.F.L., Schmidt, J.L, Schock, S.G., Simonet, F., Stoll, R.D., Tang, D., Thistle, D.E., Thorsos, E.I., Walter, D.J., Wheatcroft, R.A., 2001. An overview of SAX99: environmental considerations. IEEE J. Ocean. Eng. 26, 26–53.

Stanton, T.K., 1988. Sound scattering by cylinders of finite length: I. Fluid cylinders. J. Acoust. Soc. Am. 83, 55–63.

Stanton, T.K., 1989. Sound scattering by cylinders of finite length: III. Deformed cylinders. J. Acoust. Soc. Am. 86, 691–705.

Stanton, T.K., 1990. Sound scattering by spherical and elongated shelled bodies. J. Acoust. Soc. Am. 88, 1619–1633.

Stanton, T.K., Chu, D., 1992. Sound scattering by rough elongated elastic objects: II. Fluctuations of scattered field. J. Acoust. Soc. Am. 92, 1665–1678.

Twardowski, M.S., Sullivan, J.M., Donaghay, P.L., Zaneveld, J.R.V., 1999. Microscale quantification of the absorption by dissolved and particulate material in coastal waters with an ac-9. J. Atmos. Ocean. Tech. 16, 691–701.